metry to the reversal process with, in particular, N → R transitions resulting from the appearance of a reverse toroidal field first at high latitudes in the core. This process may be visualized if one considers the sequence displayed in Fig. 2 to run from left to right and right to left for R → N and N → R transitions, respectively.

The model presented here, being in essence phenomenological, predicts observable behavior which need not correspond uniquely to a cyclone-driven reversal process in the core and, if substantiated, will serve primarily as a constraint to the hydromagnetic behavior governing polarity transitions.

KENNETH A. HOFFMAN*
Department of Geological Sciences,
University of California,
Santa Barbara 93106

References and Notes

1. T. Nagata, *J. Geomagn. Geoelec.* **21**, 701 (1969).
2. F. E. M. Lilley, *Proc. R. Soc. London Ser. A* **316**, 153 (1970).
3. S. I. Braginskii, *J. Exp. Theor. Phys.* **47**, 1084 (1964) [English translation: *Sov. Phys. JETP* **20**, 726 (1965)].
4. E. N. Parker, *Astrophys. J.* **158**, 815 (1969).
5. E. H. Levy, *ibid.* **171**, 621 (1972); *ibid.*, p. 635; *ibid.* **175**, 573 (1972).
6. F. Krause and K.-H. Radler, in *Solar Magnetic Fields*, R. Howard, Ed. (Springer-Verlag, New York, 1971), p. 770.
7. P. Dagley and E. Lawley, *Geophys. J. R. Astron. Soc.* **36**, 577 (1974).
8. R. Dodson, J. R. Dunn, M. Fuller, I. Williams, H. Ito, V. A. Schmidt, Y. M. Wu, *ibid.*, in press.
9. K. M. Creer and Y. Ispir, *Phys. Earth Planet. Inter.* **2**, 283 (1970).
10. J. Hillhouse and A. Cox, *Earth Planet. Sci. Lett.* **29**, 51 (1976).
11. P. Steinhauser and S. A. Vincenz, *ibid.* **19**, 113 (1973).
12. A. Cox, *Rev. Geophys. Space Phys.* **13**, 35 (1975).
13. J. R. Dunn *et al.*, *Science* **172**, 840 (1971).
14. P. Dagley and R. L. Wilson, *Nature (London) Phys. Sci.* **232**, 16 (1971).
15. N. D. Watkins, *Geophys. J. R. Astron. Soc.* **17**, 121 (1969).
16. E. E. Larson, D. E. Watson, W. Jennings, *Earth Planet. Sci. Lett.* **11**, 391 (1971).
17. H. Ito and M. Fuller, in *Paleogeophysics*, S. K. Runcorn, Ed. (Academic Press, New York, 1970), p. 133.
18. N. Niitsuma, *Tohoku Univ. Sci. Rep. Ser. 2 (Geol.)* **43**, 1 (1971).
19. G. Z. Gurary, *Proc. Int. Assoc. Geomagn. Aeron. Assembly Kyoto* (1973), p. 319.
20. I thank the National Science Foundation for making it possible for me to work during the summer months with the rock magnetism and paleomagnetism group at the University of California at Santa Barbara, the members of which share interests similar to my own. Support was provided by the foundation's Research Opportunities for Small-College Faculty Program through NSF grant DES75-15541. I thank M. Fuller for many helpful discussions and a critical review of the manuscript.

* Permanent address: Physics Department, California Polytechnic State University, San Luis Obispo 93407.

14 September 1976; revised 11 January 1977

Lithium-Sodium Beta Alumina: First of a Family of Co-ionic Conductors?

Abstract. *Lithium-sodium beta alumina having a lithium/sodium ratio greater than about 1 appears to be the first generally useful lithium superionic conductor that has been reported. It exhibits strikingly nonlinear ion exchange properties and may presage the discovery of similar co-ionic interactions in other superionic conductors. The properties of lithium-sodium beta alumina are discussed in relation to current concepts of ionic interaction and distribution in the beta alumina conduction plane.*

Since Yao and Kummer (*1*) reported the high conductivity of Na^+ in Na^+ beta alumina, considerable effort has been directed toward identifying a comparable Li^+ conductor. Lithium is the most reducing of the alkali metals and also has the lowest equivalent weight. It is therefore attractive for use in compact and light rechargeable batteries. A high-conductivity Li^+ solid electrolyte would lend flexibility in the design of such energy storage systems.

A good Li^+ conductor has now been found in the form of Na^+ beta alumina in which a portion of the Na^+ is replaced by Li^+ (*2*). The result is a solid-solution Li^+-Na^+ beta alumina in which charge is carried by both monovalent cations. What is surprising is that the relative proportion of charge carried by each ion as a function of the Li^+/Na^+ ratio is extremely nonlinear. For compositions having Li^+/Na^+ greater than ~ 1, the fraction of current carried by Li^+ is nearly unity. Lithium ions move through the solid electrolyte structure without significantly altering its Na^+ content.

Numerous applications exploiting the chemical stability and high Li^+ conductivity of Li^+-Na^+ beta alumina can be imagined. But more intriguing may be the implication that similar nonlinear properties may be found generally among other superionic conductors, including those not of the beta alumina structure. We have suggested that an appropriate term for these ionic interactions would be co-ionic conductivity (*2*). Our purpose here is to report the unexpected features of Li^+-Na^+ beta alumina, their structural basis, and their implications for other co-ionic compositions.

Yao and Kummer first reported that Li^+, in addition to Ag^+, Tl^+, K^+, Rb^+, and Cs^+, can substitute for Na^+ in Na^+ beta alumina. The Li^+ exchange is curious in that a sample of pure Na^+ beta alumina equilibrated with a large excess of $LiNO_3$ at 350°C undergoes only approximately 50 percent ion exchange. The small—generally less than 0.5 percent—impurity level of Na^+ in the $LiNO_3$ melt is sufficient to maintain a Li^+/Na^+ ratio of about 1. Yao and Kummer reported preparing pure Li^+ beta alumina by equilibrating Ag^+ beta alumina, first prepared by ion exchange of Na^+ beta alumina in molten $AgNO_3$, with $LiNO_3$ saturated with LiCl.

There has been considerable disagreement over the conductivity of Li^+ beta alumina. Radzilowski *et al.* (*3*) used tracer diffusion and dielectric loss techniques to deduce the ionic conductivity of beta alumina powder in which an unspecified proportion of the Na^+ content had been replaced by Li^+. Their values, along with that reported by Whittingham and Huggins (*4*) from measurements on single crystals of beta alumina containing Li^+, are listed in Table 1. It is somewhat surprising that even though Li^+ is a smaller ion than Na^+ and might therefore be expected to diffuse more readily, the conductivity of Li^+ beta alumina is about 10 to 1400 times smaller than that of Na^+ beta alumina, which for the single-crystal form is 1.4×10^{-2} $(\text{ohm-cm})^{-1}$ at 25°C. Conductivity in Na^+ beta alumina is due to two-dimensional diffusion of Na^+ in planes that lie between close-packed oxygen layers perpendicular to the hexagonal *c*-axis (*5*). Yao and Kummer (*1*) suggested that Li^+ beta alumina is a poor conductor because Li^+ is too small for the conducting "slots" in the crystal, and as a result is displaced from the median conduction plane and attached to oxygen atoms on the wall. This explanation is consistent with measurements of the resistivity of Li^+ beta alumina as a function of pressure, which show a resistivity decrease of 5 to 6 percent at a pressure of 4 kbar (*6*).

We have examined Li^+ exchange of polycrystalline Na^+ beta alumina tubes prepared in this laboratory by a technique previously described by Powers (*7*). Our results corroborate those of Yao and Kummer. Approximately 50 percent of the Na^+ content of polycrystalline Na^+ beta alumina is replaced by Li^+ during immersion for several hours in molten $LiNO_3$ at 350° to 450°C. The composition appears to be in equilibrium with the melt, and the exchange occurs without obvious cracking or degradation of ceramic stability or strength.

What is remarkable about Na^+ beta alumina is the steep slope of its ion exchange equilibrium curve with Li^+ in molten $LiNO_3$. This must arise from interactions within the beta alumina structure, since the activities of Li^+ and Na^+ in mixed $LiNO_3$-$NaNO_3$ melts deviate only slightly from their concentrations (*8*). As a result, when 1 : 1, Li^+-Na^+ beta alumina is used in an electrochemical cell to separate two chambers, each containing molten $LiNO_3$ with which the sample has been previously equilibrated, its residual Na^+ concentration is not rapidly swept out on prolonged Li^+ passage. Instead, Li^+ ions move through the structure without substantially altering its Na^+ content. Cleaver and Rowlands (*9*) have observed similar behavior.

The resistivity of a typical specimen of 1:1 Li^+-Na^+ beta alumina was determined by a four-probe galvanostatic technique designed to distinguish intragrain and grain boundary resistivities (*10, 11*). The intragrain resistivity of 1 : 1 Li^+-Na^+ beta alumina, which approximates the single-crystal resistivity, is typically 200 ohm-cm at 25°C. Grain boundaries contribute an additional 800 ohm-cm at 25°C. Thus, the d-c resistivity of a typical polycrystalline Na^+ beta alumina tube increases by a factor of 2 to 5 when the tube is converted to 1 : 1 Li^+-Na^+ beta alumina. We have found that the total extent of Li^+ exchange in Na^+ beta alumina can be increased by multiple equilibrations with fresh $LiNO_3$ at 600°C. A maximum of 89 percent Na^+ replacement has been achieved by this method. Resistivity data in this range are incomplete, but indicate that this further exchange increases d-c resistivity by at most a factor of 2.

To demonstrate a typical electrochemical application of polycrystalline 1 : 1 Li^+-Na^+ beta alumina, a sample disk prepared by thermal exchange was incorporated into a Li/Li^+-Na^+ beta alumina/Br_2 test cell. Propylene carbonate containing $LiClO_4$ and LiBr was the liquid electrolyte, and the Li electrode was formed in situ by deposition of Li on a Ni foam substrate. No increase in cell resistance attributable to the solid electrolyte was observed during discharge at 2.2 ma per square centimeter of disk area over several days, or during subsequent recharge at a similar rate. During this time, sufficient charge was passed to replace 224 percent of the total Li^+ content of the disk.

To begin to understand the unexpected behavior of Li^+ and Na^+ ions in 1 : 1 Li^+-Na^+ beta alumina we consider the defects responsible for mass and charge transport. In most solid ionic conductors, current is carried by thermally activated migration of charged point defects, typically interstitial ions, vacancies, or impurities. In superionic conductors (*12*), typified by Na^+ beta alumina, the concentration of charge carriers and vacancies is large, and they interact to form short-range ordered regions called extended defects in which the local structure and properties are slightly modified. Nonlinear co-ionic properties are possible because chemically distinguishable mobile ions can occupy similar but nonequivalent sites in the disordered crystal.

Table 1. Conductivity of Li^+-Na^+ beta alumina. All data are single-crystal values at 298°K. The tracer diffusion and dielectric loss values are from (*3*), the a-c conductivity values from (*4*).

Method	Conductivity $[(\text{ohm-cm})^{-1}]$
Tracer diffusion*†	1.0×10^{-5}
Dielectric loss†	1.5×10^{-3}
Conductivity (a-c)†	1.3×10^{-4}
This work‡	5×10^{-3}

*The value given was extrapolated to 298°C. †The precise Li^+/Na^+ ratio in the sample was not reported; the nominal mole fraction of Li^+ was unity. ‡Li^+/Na^+ = 1.1.

The ideal atomic arrangement in Na^+ beta alumina, exclusive of the defects, has been known since 1931 from the crystal structure studies of Bragg *et al.* (*13*) and Beevers and Ross (*14*). It was not until 1971 that Peters *et al.* (*5*) established, by an investigation of the structure with modern x-ray methods, that the high conductivity is due to fast diffusion of Na^+ ions in planes of low atomic density with excess vacancies for each Na^+. Studies of the ion transport mechanism, defects, and disorder structure by x-ray diffuse scattering (*15*), neutron diffraction (*16*), and nuclear magnetic resonance (*17*) are beginning to provide a description of the defects responsible for conductivity. The extended defect in Na^+ beta alumina is a cluster of Na^+, O^{2-}, and vacancies in Beevers-Ross (BR), mid-oxygen (mO), and anti-Beevers-Ross (aBR) sites. Figure 1 describes a single ion diffusion path in Na^+ beta alumina. The sodium sites are crystallographically independent, and the shapes and depths of the potential wells and the heights of the barriers between sites may be different. The potential function in Fig. 1 is a schematic representation inferred from site occupation probabilities and symmetry (*16*). The highest barrier is indicated between mO and aBR sites, consistent with the interstitialcy mechanism proposed by Whittingham and Huggins (*18*) to explain the Nernst-Einstein correlation coefficient of about 0.6 for tracer diffusion in Na^+ beta alumina.

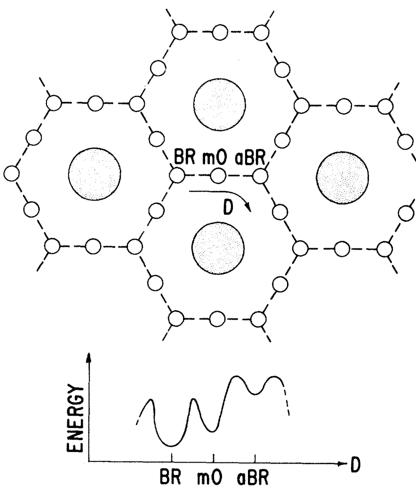

Fig. 1. Single ion diffusion path in beta alumina. Cations hop between the BR, mO, and aBR sites in an interconnected two-dimensional network between rigid oxygen pillars. The potential energy curve is a schematic representation inferred from Na^+ beta alumina site probabilities. The rate-determining step is believed to be hopping over the energy barrier between mO and aBR sites. The shapes of the potential wells in Li^+-Na^+ beta alumina are expected to be different. *D*, distance along the ionic diffusion path.

The binding energy of mobile cations in the various sites of the conduction plane is different and of order kT (where k is the Boltzmann constant and T is absolute temperature), as shown by the change in the average density of Na^+ in the sites when temperature is increased from −193°C to +600°C (*16*). Sodium ions in these sites interact differently with the surrounding crystal field, and individual asymmetry and quadrupole parameters are resolved in low-temperature single-crystal rotation patterns of the ^{23}Na nuclear magnetic resonance spectrum (*17*). Above −163°C, Na^+ ions hop rapidly between sites and the spectra merge into a single resonance peak. We believe, therefore, that electric current in beta alumina is carried by ions migrating through a sequence of energetically distinguishable sites. The potential energies of specific cations in these sites will depend on their electronic structure and ratio of ion charge to diameter. This unequal binding also accounts for the striking variation in activity coefficients of a cation (M^+) in the solid and melt observed by Yao and Kummer (*1*) for equilibria between $(MNO_3\text{-}NaNO_3)_{liquid}$ and $(M^+\text{-}Na^+ \text{ beta alumina})_{solid}$. Similar nonideal behavior is observed in solutions of strong electrolytes and in glasses (*19*).

A large concentration of charge carriers is a common structural feature of superionic conductors, and it will be interesting to examine other crystal structures for similar co-ionic compositions that may display nonlinear ionic transport. An attractive coordinate is the framework structure $M_{1+x}Zr_2Si_xP_{3-x}O_{12}$, where M = Li, Na, Ag, or K (*20*).

WALTER L. ROTH
GREGORY C. FARRINGTON
Research and Development Center,
General Electric Company,
Schenectady, New York 12301

References

1. Y. F. Y. Yao and J. T. Kummer, *J. Inorg. Nucl. Chem.* **29**, 2453 (1967).
2. G. C. Farrington and W. L. Roth, *Superionic Conductors*, G. D. Mahan and W. L. Roth, Eds. (Plenum, New York, 1977), p. 418.
3. R. H. Radzilowski, Y. F. Yao, J. T. Kummer, *J. Appl. Phys.* **40**, 4716 (1969).
4. M. S. Whittingham and R. A. Huggins, *Natl. Bur. Stand. (U.S.) Spec. Publ. No. 364* (1972), p. 139.
5. C. R. Peters, M. Bettman, J. W. Moore, M. D. Glick, *Acta Crystallogr. Sect. B.* **27**, 1826 (1971).
6. R. H. Radzilowski and J. T. Kummer, *J. Electrochem. Soc.* **118**, 714 (1971).
7. R. W. Powers, *ibid.* **122**, 490 (1975).
8. C. Sinistri and P. Franzosini, *Ric. Sci. Parte 2 Sez.* **A 3**, 449 (1963).
9. B. Cleaver and G. Rowlands, personal communication.
10. G. C. Farrington, *J. Electrochem. Soc.* **121**, 1314 (1974).
11. ———, *ibid.* **123**, 833 (1976).
12. M. J. Rice and W. L. Roth, *J. Solid State Chem.* **4**, 294 (1972).
13. W. L. Bragg, C. Gottfried, J. West, *Z. Kristallogr. Kristallgeom. Kristallphys. Kristallchem.* **77**, 225 (1931).
14. C. A. Beevers and M. A. S. Ross, *ibid.* **97**, 59 (1937).
15. J. P. Boilot, G. Collin, R. Comes, J. Thery, R. Collongues, A. Guinier, in *Superionic Conductors*, G. D. Mahan and W. L. Roth, Eds. (Plenum, New York, 1977), p. 243.
16. W. L. Roth, F. Reidinger, S. J. LaPlaca, in *ibid.*, p. 223.
17. W. Bailey, S. Blowinkowski, H. S. Story, W. L. Roth, *J. Chem. Phys.* **64**, 4126 (1976).
18. M. S. Whittingham and R. A. Huggins, *ibid.* **54**, 414 (1971).
19. M. E. Milberg, in *Fast Ion Transport in Solids*, W. vanGool, Ed. (North-Holland, Amsterdam, 1973), p. 373.
20. H. Y-P. Hong, *Mater. Res. Bull.* **11**, 173 (1976).

20 September 1976; revised 18 February 1977

Radioimmunoassay for Abnormal Hemoglobins

Abstract. *A sensitive and specific radioimmunoassay has been developed for the identification or quantification of the human hemoglobin variants S, C, D-Los Angeles, E, G Philadelphia, Russ, O Arab, Beograd, J Paris I, G San Jose, Q Iran, Korle Bu, and F Malta I. In the immunoassay, monospecific antibody preparations are used which recognize the single amino acid substitution in the variant polypeptide chain and do not cross-react with normal hemoglobins or hemoglobin variants containing a different amino acid exchange at the same position.*

Hemoglobin (Hb) from normal individuals and those with various hemoglobinopathies has been the subject of extensive structural, functional, and genetic investigations. At the present time, more than 275 different hemoglobin variants have been discovered (*1*). In the majority of these variants, there is a single amino acid substitution in one of the two hemoglobin subunits. Generally these mutants are rare in the population and have no clinical consequences in heterozygous individuals, although four abnormal hemoglobins (S, C, D, and E) are frequently observed in certain populations and can be associated with pathological manifestations (*2*). Because the common method of detection and preliminary identification of variants is based on comparative electrophoretic differences between the abnormal and normal proteins, most of those reported have an amino acid exchange involving residues of unlike charge. However, since many different abnormal hemoglobins have similar or identical mobilities, conclusive identification requires structural analyses.

We have developed a radioimmunoassay (RIA) system with monospecific antiserums capable of recognizing and, if necessary, quantifying hemoglobin variants in red cell hemolyzates. Included in our study are the four most prevalent abnormal hemoglobins (S, C, D, and E), as as well as G Philadelphia, which is probably the most common α-chain variant in the black population in the United States (*3*). These and other hemoglobin variants for which RIA's have been developed are listed in Table 1.

Blood samples for isolation of the hemoglobin variants were obtained from patients whose abnormal hemoglobin had been structurally characterized. Methods of isolation included column chromatography on diethylaminoethyl (DEAE)-Sephadex, DEAE-cellulose, carboxymethyl (CM)-cellulose, and CM-Sephadex, with developers and conditions as described (*4*). Each preparation was analyzed for purity by starch-gel electrophoresis at *p*H 9.0 (*5*). All isolated hemoglobins migrated as single bands free of hemoglobins A, F, or A_2, except for HbE and HbO Arab which could not be completely separated from HbA_2.

Antiserums to the variants were prepared in white New Zealand rabbits with Freund's complete adjuvant according to the dose, route, and schedule outlined (*6*). Antiserum to HbE was produced in chickens by a similar immunization schedule (*7*). Antibody preparations were made monospecific for the variants by absorption with HbA conjugated to AH-Sepharose activated with glutaraldehyde (*8*); antiserum to HbF Malta I was absorbed with HbF ($^{G}\gamma$). In addition, antiserums to HbE and HbO Arab were absorbed with HbA_2. After absorption, the preparations of antiserums were concentrated approximately tenfold by negative-pressure dialysis.

The antibody titers were measured by determining the extent of binding of the absorbed antiserums with the corresponding ^{125}I-labeled variant hemoglobin; similar titrations were also made with ^{125}I-labeled normal hemoglobins (A, A_2, and F) to confirm the absence of cross-reactivity. The principle of the RIA is based on the separation of free and bound ^{125}I-labeled antigen by the addition of ammonium sulfate solution. Details of this method have been described (*6*). After absorption, each variant antiserum precipitated only the ^{125}I-labeled hemoglobin variant and did not react with labeled HbA, HbA_2, or HbF, in the case of antiserum to HbF Malta I.

In order to further ensure the specificity of the antiserum for each particular mutant, standard RIA inhibition assays were performed. In these tests, the tubes contained a constant volume of antiserum, which was diluted to yield approximately 35 percent precipitation of the ^{125}I-labeled hemoglobin variant. Increments of unlabeled normal or variant hemoglobins were then added to the tubes. After incubation for 1 hour at room temperature, a constant quantity (0.1 μg) of the labeled hemoglobin variant was added to all tubes. Under these conditions, a competition reaction is established between the labeled and unlabeled hemoglobin for the available antibody-combining sites. If a sufficient amount of the homologous unlabeled Hb antigen is present, the antibody-combining sites become saturated, and the ^{125}I-labeled antigen is located in the supernatant fraction after the addition of ammonium sulfate solution. The representative inhibition curve (Fig. 1a) shows that the homologous antigen (HbS) competitively blocked the binding between antiserum to HbS and ^{125}I-labeled HbS in quantities ranging from 0.1 to 10.0 μg, while HbA, HbF, and HbA_2 did not inhibit the reaction at any of these concentrations.

The feasibility of using the RIA to identify and quantify abnormal hemoglobins in red blood cell hemolyzates was evaluated with the use of antiserums to